AIP | Applied Physics Letters

Thermal transport through superlattice solid-solid interfaces

Sohail Murad and Ishwar K. Puri

Articles you may be interested in

Few layer graphene based superlattices as efficient thermal insulators
Appl. Phys. Lett. **103**, 141905 (2013); 10.1063/1.4824013

Heat conduction across a solid-solid interface: Understanding nanoscale interfacial effects on thermal resistance
Appl. Phys. Lett. **99**, 013116 (2011); 10.1063/1.3607477

Interfacial thermal transport between nanotubes
J. Appl. Phys. **106**, 084302 (2009); 10.1063/1.3245388

Unsteady nanoscale thermal transport across a solid-fluid interface
J. Appl. Phys. **104**, 064306 (2008); 10.1063/1.2978245
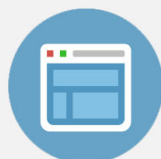
Thermal transport across nanoscale solid-fluid interfaces
Appl. Phys. Lett. **92**, 133105 (2008); 10.1063/1.2905281

Thermal transport through superlattice solid-solid interfaces

Sohail Murad[1] and Ishwar K. Puri[2,a)]
[1]Department of Chemical Engineering, University of Illinois at Chicago, Chicago, Illinois 60607, USA
[2]Department of Engineering Science and Mechanics, Virginia Polytechnic Institute and State University,
Blacksburg, Virginia 24061, USA

Using molecular dynamics, we consider the thermal resistances of superlattices consisting of varying numbers of distinct nanolayers of two different materials. These are placed between two water reservoirs at uniform hot and cold temperatures. The interfacial resistances produced between different solid layers can lead to significantly lower heat transfer for a specified temperature difference. Such a large reduction in thermal transport cannot be explained by the interfacial resistance alone. In addition to the interfacial resistance between two adjacent superlattice layers, the relatively wide thermal boundary layers that are produced adjacent to the interfaces introduces a supplementary resistance. © 2009 American Institute of Physics. [DOI: 10.1063/1.3197012]

Phonon scattering at nanoscale interfaces[1–4] produces a thermal contact resistance that impedes the heat flux.[5,6] Thus, the nature of an interface has an important influence on thermal transport,[7–10] e.g., through the formation of a thermal boundary layer adjacent to it.[10] Combinations of thermal resistances in multilayered solid materials should decrease the heat transferred through their bulk as compared to, say, a homogeneous solid. Since the thermal resistance is inversely proportional to the interface temperature,[11] the impedance to heat transfer should decrease with it. Interface effects cannot alone explain the reduction in the thermal conductivities[12,13] of superlattices as compared to alloys with the same composition.[14] We use molecular dynamics (MD) simulations to examine some unresolved issues by investigating model silicon-water like superlattice systems.

MD is applicable to phonon transport in nonmetallic solids above their Debye temperatures T_D.[14] We consider a system that consists of 4224 particles in the basic cyclically replicated parallelepiped that is described in Fig. 1. It consists of two solid 6.5 nm walls that separate 4 nm wide fluid reservoirs.[8,10] Both walls consist of 3072 solid atoms in the form of $4 \times 4 \times 6$ unit cells that contain eight atoms. The fluid reservoirs contain 1152 uniformly distributed water molecules at a density of 975 kg/m^3. The solid atoms are of four siliconlike materials M_i, namely, Si (or M_1) or its close variants M_2, M_3, and M_4. These are placed at the normal equilibrium sites for a silicon crystal. We provide the molecules with initial Gaussian velocity distributions[15] which impart different high and low temperatures, $T_h \gtrsim T_D \approx 645$ K (for a nonmetallic Si crystal[16]) and T_c to the fluid reservoirs.

We simulate three solid-fluid systems with (1) homogenous walls consisting of a single material M_i, (2) composite walls comprised of a single Si-$M_{i,i=2,3,4}$ bilayer, and (3) multilayer walls (superlattices) consisting of six Si-$M_{i,i=2,3,4}$ composite layers. Figure 1 schematically describes the latter two systems with Si-M_4 layers. In all cases, the overall system length $L_y=21$ nm, and its height L_y and width L_z are both 2.172 nm.

We have employed the simulation algorithm, described elsewhere,[15,17–19] to investigate various interfacial heat and mass transport problems.[8–10,15,20–24] Intermolecular interactions follow the potential $u_{ij} = 4\varepsilon_{ij}[(\sigma_{ij}/r_{ij})^{12} - (\sigma_{ij}/r_{ij})^6] + q_iq_j/r_{ij}$, where σ_{ij} and ε_{ij} denote the Lennard-Jones (LJ) interaction parameters, r_{ij} the scalar distance between sites i and j, and q_i and q_j charges on sites when applicable. The parameters σ and ε, presented in Table I, represent experimental geometries, energies of ion-water complexes, and of solvation[25] for (1) water (modeled with the SPC potential)[10,26] and (2) Si (or M_i) wall atoms modeled as LJ sites.[8,21,22]

We emulate the coordinated tetrahedral bonded Si structure by tethering the M_i atoms to their equilibrium sites using a simple harmonic potential with a 61.7 J m^2 spring constant. This leads to an ideal vibrational frequency for a simple harmonic oscillator of 19 304 cm^{-1}. Because the tethered molecules interact strongly with neighboring atoms, the actual vibrational frequency is lower than this value. The parameter values for the hypothetical M_i solids are identical to those for Si except that $\sigma_2=1.067\sigma_{Si}$, $\sigma_3=1.1167\sigma_{Si}$, and $\sigma_4=1.167\sigma_{Si}$ for the interactions of M_1, M_2, and M_3 with other M_i atoms. All M_i atoms interact identically with water, since our purpose is to focus on the solid-solid resistances.

The simulated cases are summarized in Table II. Segmenting the simulation domain into $138\Delta x \approx 0.152$ nm thick transverse strips along L_x provides averaged temperatures in
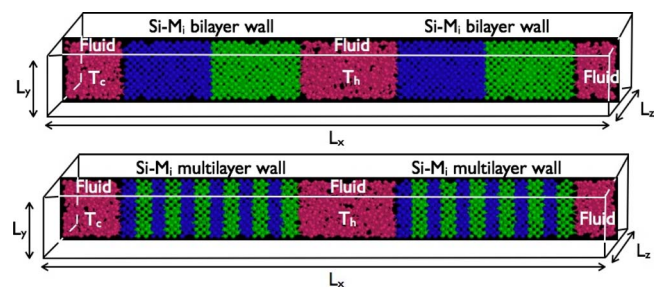

FIG. 1. (Color online) Schematic diagram of the domain based on an arbitrary simulation for systems with bilayer and six-layer composite Si (or M_1)-M_i superlattice walls. Periodic boundary conditions apply on all six faces of the basic cyclically replicated parallelepiped. The domain dimensions are $L_x=20.99$ nm and $L_y=L_z=2.172$ nm.

a)Author to whom correspondence should be addressed. Electronic mail: ikpuri@vt.edu.

TABLE I. Values of the Lennard-Jones interactions parameters σ, ε, and q. Cross interactions are modeled based on Lorentz–Berthelot mixing rules.

	σ 10^{-10} m	ε KJ mol^{-1}	q e
O	3.17	0.65	−0.82
H	0	0	0.41
Si	4.028	0.87	0

these local sections for each case. Figure 2 presents the temperature profiles for Cases I and Ia. These are converged within 2% of their reported local values over the last 2 $\times 10^6$ simulation steps. The temperature distribution for Case I reveals thermal boundary layers adjacent to the solid-fluid and solid-solid interfaces that form resistances which lower the effective thermal conductivity.[10] The boundary layer thickness $\delta_t \approx 2\Delta x$ or 0.3 nm is roughly a single atomic layer wide. Since it is identical in the Si and M_4 layers, the heat flux Q through the composite wall is constant. Using the empirical Fourier law $Q = -k\nabla T$ where k denotes the thermal

conductivity, the lower effective k for the Si wall is apparent through the steeper ∇T profile as compared to that for M_4. Placing thermal resistances in series in a composite six-layer Si-M_4 wall further distorts the profile, since phonon scattering now occurs at multiple Si-M_4 interfaces, decreasing Q and thus k, as illustrated in Table II.

For the LJ model, increasing σ augments the intermolecular interactions between two neighboring M_i atoms or sites, i.e., a decrease in the interparticle distance enhances thermal transport. The heat flux through monolayer walls of a single material increases as $Q \propto \sigma^{3.64}$, i.e., thermal transport scales roughly with the material atomic volumes. Thus, varying the thickness of a layer should not influence this effect. Table II compares the relative heat flux (normalized against Case III) Q/Q_{III} for each case as a function of the wall composition and overall temperature difference across it. A $\sim 17\%$ increase in molecular size (for M_4—Case X and over Si—Case VII) leads to a $\sim 80\%$ increase in Q for a 645 K temperature difference across the wall. A six-layer Si-M_4 wall conducts less heat than a corresponding bilayer composite wall. The heat transferred across a six-layer wall is 5%
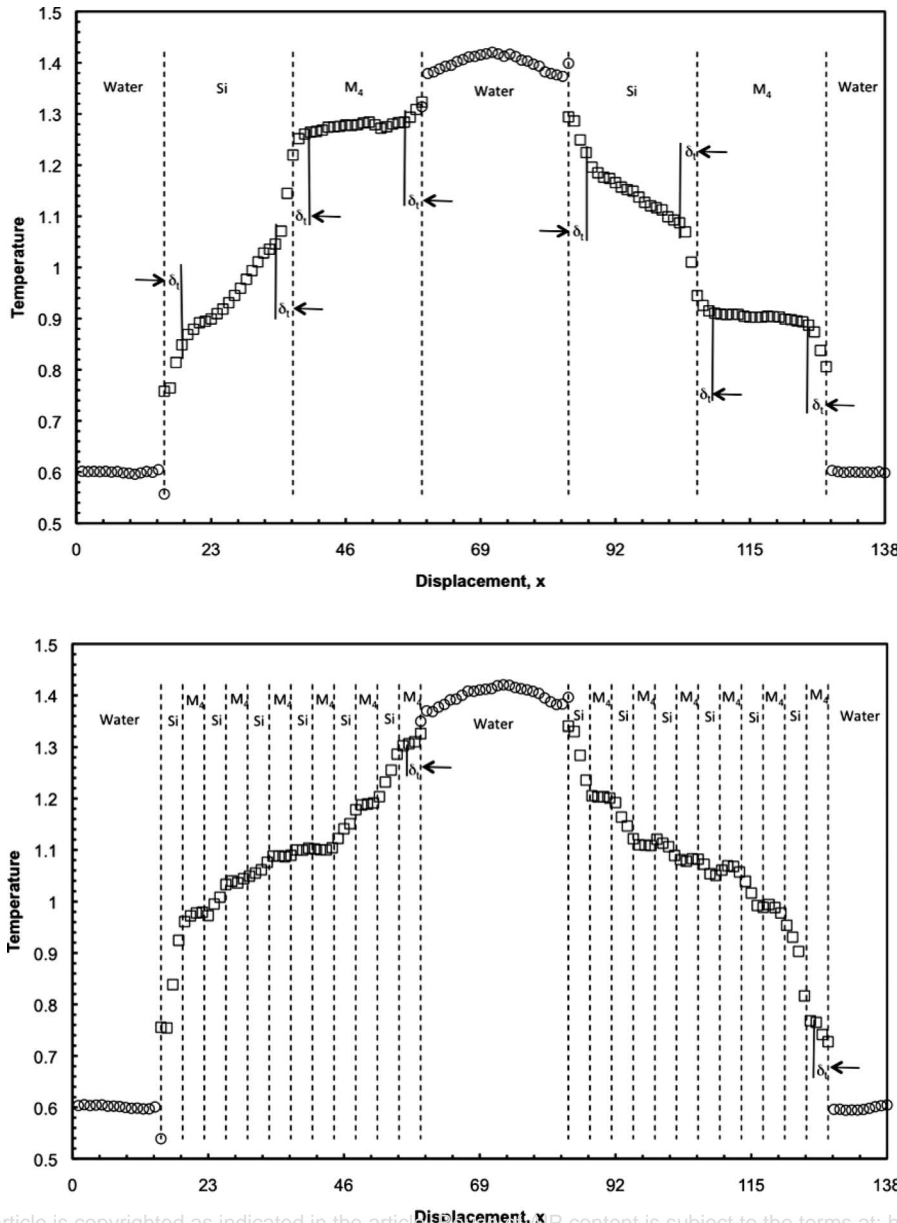

FIG. 2. The temperature profiles for Cases I and Ia. The segment numbers on the abscissa multiplied by 0.152 nm return the axial distance. The dimensionless temperature ordinate multiplied by 806.46 K provides the local temperature.

TABLE II. List of simulation cases corresponding to the materials comprising the solid superlattice walls, numbers of composite $(M_i - M_j)$ layers in each wall, imposed hot- and cold-side fluid reservoir temperatures T_h and T_c, simulated heat flux Q through the superlattice walls, and the ratio of Q to the flux for a base case (III). Cases VII–X are for homogeneous walls.

Case	Material 1	Material 2	Composite bilayers	T_h (K)	T_c (K)	$Q \times 10^7$ (W)	Q/Q_{III}
I	Si(M_1)	M_4	1	1210	403	2.69	1.05
Ia	Si(M_1)	M_4	6	1210	403	2.55	0.99
II	Si(M_1)	M_4	1	1169	444	2.64	1.03
IIa	Si(M_1)	M_4	6	1169	444	2.50	0.98
III	Si(M_1)	M_4	1	1129	484	2.57	1.00
IIIa	Si(M_1)	M_4	6	1129	484	2.19	0.85
IV	Si(M_1)	M_4	1	1089	524	2.27	0.88
IVa	Si(M_1)	M_4	6	1089	524	1.78	0.69
V	Si(M_1)	M_4	1	1048	565	2.15	0.84
Va	Si(M_1)	M_4	6	1048	565	1.28	0.50
VI	Si(M_1)	M_2	1	1129	484	2.19	0.85
VIa	Si(M_1)	M_2	6	1129	484	2.19	0.85
VII	Si(M_1)	⋯	⋯	1129	484	2.02	0.79
VIII	M_2	⋯	⋯	1129	484	2.57	1.00
IX	M_3	⋯	⋯	1129	484	2.86	1.11
X	M_4	⋯	⋯	1129	484	3.63	1.41

smaller than the flux across a bilayer wall when the temperature difference across it is 806 K (Case Ia). For a 645 K difference the flux is reduced by 15% (Case IIIa) but its decrease is 41% at 484 K (Case Va). These changes in the thermal conductivity[12,13] cannot be accounted for by the interface resistance alone.[14] We attribute the decrease in k also to the thermal boundary layers around the contact interface between two solid crystals. Lowering the temperature difference makes a multilayer wall less effective in transferring heat, since the thermal impedance is sensitive to the temperature difference and the interfacial temperature.

In summary, we show that impedance to nanoscale thermal transport is enhanced by subnanometer thermal boundary layers at the interfaces of superlattices due to two effects, namely, (1) the interfacial resistance between two solid phases of a superlattice and (2) the thermal boundary layers that are formed within each phase adjacent to these interfaces. This observation can have significant design implications for semiconductor and related electronic devices that dissipate energy as heat. For example, depending upon the desired outcome, it would be advantageous to have composite films constructed in several alternating layers to inhibit heat transfer, but have fewer layers present if the thermal transport is to be enhanced.

[1] L. J. Challis, J. Phys. C **7**, 481 (1974).
[2] J.-L. Barrat and F. Chiaruttini, Mol. Phys. **101**, 1605 (2003).
[3] C. Oligschleger and J. C. Schon, Phys. Rev. B **59**, 4125 (1999).
[4] P. A. E. Schoen, B. Michel, A. Curioni, and D. Poulikakos, Chem. Phys. Lett. **476**, 271 (2009).
[5] E. T. Swartz and R. O. Pohl, Rev. Mod. Phys. **61**, 605 (1989).
[6] P. L. Kapitza, J. Phys. (USSR) **4**, 181 (1941).
[7] G. Balasubramanian, S. Banerjee, and I. K. Puri, J. Appl. Phys. **104**, 064306 (2008).
[8] S. Murad and I. K. Puri, Appl. Phys. Lett. **92**, 133105 (2008).
[9] S. Murad and I. K. Puri, Chem. Phys. Lett. **467**, 110 (2008).
[10] S. Murad and I. K. Puri, Chem. Phys. Lett. **476**, 267 (2009).
[11] A. F. Khater, J. Phys. Colloq. **39**, C6 (1978).
[12] S. M. Lee, D. G. Cahill, and R. Venkatasubramanian, Appl. Phys. Lett. **70**, 2957 (1997).
[13] T. Borca-Tasciuc, W. L. Liu, J. L. Liu, T. F. Zeng, D. W. Song, C. D. Moore, G. Chen, K. L. Wang, M. S. Goorsky, T. Radetic, R. Gronsky, T. Koga, and M. S. Dresselhaus, Superlattices Microstruct. **28**, 199 (2000).
[14] D. G. Cahill, W. K. Ford, K. E. Goodson, G. D. Mahan, A. Majumdar, H. J. Maris, R. Merlin, and S. R. Phillpot, J. Appl. Phys. **93**, 793 (2003).
[15] M. P. Allen and D. J. Tildesley, *Computer Simulation of Liquids* (Clarendon, Oxford, 1987).
[16] H.-M. Kagaya, T. Soma, and M. R. Brozel, in *Properties of Crystalline Silicon*, edited by R. Hull (The Institution of Engineering and Technology, London, U.K., 1999), pp. 151–152.
[17] S. Murad and J. Lin, Chem. Eng. J. **74**, 99 (1999).
[18] S. Murad and J. Lin, Ind. Eng. Chem. Res. **41**, 1076 (2002).
[19] D. J. Evans and S. Murad, Mol. Phys. **34**, 327 (1977).
[20] S. Banerjee, S. Murad, and I. K. Puri, Chem. Phys. Lett. **434**, 292 (2007).
[21] S. Murad and I. K. Puri, Nano Lett. **7**, 707 (2007).
[22] S. Murad and I. K. Puri, Phys. Fluids **19**, 128102 (2007).
[23] I. G. Tironi, R. Sperb, P. E. Smith, and W. F. Vangunsteren, J. Chem. Phys. **102**, 5451 (1995).
[24] H. J. C. Berendson, J. Postma, and W. F. van Gunsteren, in *Intermolecular Forces*, edited by B. Pullman (Reidel, Dordecht, 1981).
[25] J. Chandrasekhar, S. F. Smith, and W. L. Jorgensen, J. Am. Chem. Soc. **106**, 3049 (1984).
[26] R. O. Watts, Mol. Phys. **28**, 1069 (1974).